

# SCIENTIFIC REPORTS

OPEN

## Optimal leaf water status regulation of plants in drylands

Gregor Ratzmann<sup>1,2</sup>, Liubov Zakharova<sup>3</sup> & Britta Tietjen<sup>1,2,4</sup>

Leaf water potential regulation is a key process in whole plant and ecosystem functioning. While low water potentials induced by open stomata may initially be associated with greater CO<sub>2</sub> supply and a higher water flux from the rhizosphere to the canopy, they also inhibit cell growth, photosynthesis and ultimately water supply. Here, we show that plants regulate their leaf water potential in an optimal manner under given constraints using a simple leaf water status regulation model and data from a global dryland leaf water potential database. Model predictions agree strongly with observations across locations and species and are further supported by experimental data. Leaf water potentials non-linearly decline with soil water potential, underlining the shift from maximizing water supply to avoiding stress with declining water availability. Our results suggest that optimal regulation of the leaf water status under varying water supply and stress tolerance is a ubiquitous property of plants in drylands. The proposed model moreover provides a novel quantitative framework describing how plants respond to short- and long-term changes in water availability and may help elaborating models of plant and ecosystem functioning.

Leaves form an important component in the nexus of the terrestrial water and carbon cycle. They are the loci of CO<sub>2</sub> uptake and act as controlling valves for the water flux through the entire plant. Within this cascade of uptake, transport and exchange, the regulation of a plants leaf water status is a key process because it is intrinsically linked to many whole-plant functioning processes. These processes include stomatal conductance and thus CO<sub>2</sub> uptake<sup>1</sup>, canopy water supply<sup>2</sup>, xylem functioning<sup>3</sup> and the growth of cells and ultimately organs<sup>4</sup>. Being able to understand and quantitatively describe how a plant regulates its leaf water status in response to changing water availability is therefore a key element in understanding and describing whole plant functioning.

The links between leaf water status regulation and other processes are complex and best considered sequentially. When a plant opens its stomata to take up carbon dioxide it inevitably accepts a loss of water through transpiration. The consequent decline in leaf water content leads to a decline in the cellular pressure and osmotic potentials and thus in the bulk leaf water potential  $\psi_L$ , which we define as the key variable describing leaf water status. This decline in turn initiates an intercellular water flux through xylem conduits from the roots to the leaves<sup>5</sup>. Considering the whole pathway from the soil to the atmosphere water thus follows declining water potentials which gradually drop from the rhizosphere to the leaves<sup>3,5</sup>. This water flux is commonly described by Darcy's Law or in analogy to an electric current<sup>2,6</sup> and can be formalized as

$$Q = k|\psi_L - \psi_S| \quad (1)$$

Here,  $Q$  ( $\text{m}^3 \text{s}^{-1} \text{plant}^{-1}$ ) is the total water flux through a plant per time,  $k$  ( $\text{m}^3 \text{s}^{-1} \text{MPa}^{-1} \text{plant}^{-1}$ ) is the plant's bulk conductance to liquid water,  $\psi_L$  (MPa) is the plants bulk leaf water potential, and  $\psi_S$  (MPa) is the bulk plant available soil water potential. The absolute value of the gradient  $\psi_L - \psi_S$  is taken because leaf and soil water potentials are smaller than 0 and  $\psi_L$  is typically lower than  $\psi_S$  when the plant actively controls transpiration.

Everything else being equal on the right side of Eq. (1) it predicts that the water flux from soil to leaves should increase and hence improve the leaf water supply with decreasing  $\psi_L$ . Moreover, stomatal opening, which allows more CO<sub>2</sub> to enter the leaves, will lead to lower  $\psi_L$  through transpiration. Low leaf water potentials in mesophyll cells initiate stomatal closure<sup>7</sup> and thus mediate the positive effect on CO<sub>2</sub> uptake. At the same time, a low leaf water potential first inhibits overall growth processes<sup>4,8,9</sup>, because cell wall expansion and consequently cell division is directly dependent on cell turgor pressure. Further declining leaf water potentials then start

<sup>1</sup>Freie Universität Berlin, Institute of Biology, Altensteinstraße 34, 14195, Berlin, Germany. <sup>2</sup>Freie Universität Berlin, Dahlem Centre of Plant Sciences, 14195, Berlin, Germany. <sup>3</sup>Department of Ecosystem Modelling, University of Göttingen, Büsgenweg 4, 37077, Göttingen, Germany. <sup>4</sup>Berlin Brandenburg Institute of Advanced Biodiversity Research (BBIB), 14195, Berlin, Germany. Correspondence and requests for materials should be addressed to G.R. (email: [gregor.ratzmann@gmail.com](mailto:gregor.ratzmann@gmail.com))

Received: 26 March 2018

Accepted: 14 February 2019

Published online: 06 March 2019

inhibiting photosynthesis<sup>10</sup> and lead to turgor-induced stomatal closure<sup>7</sup>, which will reduce the leaf-level CO<sub>2</sub> supply. Moreover, a decline in leaf water potentials corresponds to declining xylem water potentials throughout the whole plant<sup>5,6</sup>. This, in turn, brings about a rapid, non-linear drop in xylem hydraulic conductance caused by xylem embolism, which will also lead to a decline of  $k$  in Eq. (1), ultimately leading to a decline in canopy water supply<sup>3,11</sup>.

The plant is consequently faced with the challenge of, on the one hand, allowing the leaf water potential  $\psi_L$  to drop to a point where it can still take up CO<sub>2</sub> and maintain a water flux from the soil to the leaves, while, on the other hand, avoiding leaf water potentials that will inhibit its growth and assimilation and lead to a disruption of the canopy water supply<sup>12,13</sup>. This challenge has to be solved by each plant for a given structural and functional configuration<sup>13</sup>, such as leaf to root area ratio, plant height, and xylem conductance, and for variable environmental constraints<sup>14</sup>, such as air vapor pressure deficit or irradiation. The means by which a plant can regulate its leaf water potential are stomatal opening and closure and accumulation of osmolytes in leaf cells.

In studies of the leaf and soil water potential relationship the approximation is often made that predawn leaf water potential ( $\psi_{pd}$ ,  $\psi_L$  at predawn) is a close proxy for soil water potential and that leaf water potentials at midday ( $\psi_m$ ,  $\psi_L$  at midday) are a proxy for  $\psi_L$ <sup>15</sup>. We will use the approximations  $\psi_L \approx \psi_m$  and  $\psi_S \approx \psi_{pd}$  throughout this study. In fact, a plant rapidly reduces its  $\psi_m$  as the soil dries and  $\psi_{pd}$  declines<sup>15–17</sup>. This relationship between  $\psi_m$  and  $\psi_{pd}$  has been described using linear regressions<sup>15</sup>, however, without satisfyingly describing the initial rapid drop of  $\psi_m$  with declining  $\psi_{pd}$ . The decline of  $\psi_m$  continues until a critical point  $\psi_{crit}$  is reached, where  $\psi_m = \psi_{pd}$ <sup>16</sup>, at which the driving gradient from soil to leaves (Eq. (1)) has vanished and stomata are entirely closed<sup>16,18</sup>. Moreover, maintaining  $\psi_m$  above  $\psi_{crit}$  as long as  $\psi_{pd} > \psi_{crit}$  prevents the plant from embolism in leaf and stem conduits<sup>19,20</sup>. Values of  $0 > \psi_m > \psi_{crit}$  thus form the range of water potentials which are under the active control of the plant.

Despite considerable advancements in quantifying leaf water status and stomatal regulation<sup>12,15,16</sup>, a quantitative description of the dilemma that a plant is facing when regulating its leaf water potential is still missing.

Here, we propose a quantitative description of leaf water status regulation under drying soil conditions using a simple model and hypothesize that plants regulate their leaf water potential optimally based on the described tradeoff rather than on a purely descriptive linear regression<sup>15</sup>. We test the model using a database of concurrent observations of  $\psi_{pd}$  and  $\psi_m$  for global drylands. We additionally test the model against observations of  $\psi_{pd}$  and  $\psi_m$  during a soil drying experiment for several woody species conducted by Meinzer *et al.*<sup>16</sup>. This test additionally provides a benchmark of the model's applicability beyond drylands.

## Theoretical Framework

A drop in a plant's leaf water potential is an inevitable consequence of stomatal opening and transpiration. However, low leaf water potentials come at the cost of low growth and assimilation efficiencies and potential negative effects on the leaf supplying conduits. We suggest that this tradeoff can be described as follows (Fig. 1). The first criterion, namely that the plant needs to maximize the gradient  $\psi_m - \psi_{pd}$  and thus canopy water and CO<sub>2</sub> supply, can be expressed as

$$\lambda = \frac{\psi_m - \psi_{pd}}{\psi_m} \quad (2)$$

The second criterion, namely to keep  $\psi_m$  as high as possible, is based on the fact that the more  $\psi_m$  approaches  $\psi_{crit}$ , the more desiccation-stressed this leaf is and can be written as

$$\gamma = \frac{\psi_{crit} - \psi_m}{\psi_{crit}} \quad (3)$$

Relating both distances ( $\psi_m - \psi_{pd}$  and  $\psi_{crit} - \psi_m$ ) to a reference value ( $\psi_m$  in Eq. (2) and  $\psi_{crit}$  in Eq. (3)) has the effect that both criteria  $\lambda$  and  $\gamma$  are made dimensionless. An optimal leaf water potential for any soil water potential should thus maximize

$$\chi = \lambda + \gamma \quad (4)$$

with the underlying simple assumption that both criteria are equally weighted, and consequently suffice

$$\frac{d\chi}{d\psi_m} = 0 \quad (5)$$

The leaf water potential which satisfies Eq. (5) for any  $\psi_{pd}$  has two solutions, one with a positive sign and one with a negative sign. The latter is appropriate in this case and given by

$$\psi_m = -\sqrt{\psi_{crit}\psi_{pd}} \quad (6)$$

Equations (2–6) predict that for any given  $\psi_{pd}$  there is one optimal  $\psi_m$  (Fig. 1a). Increasing  $\psi_m$  beyond this value would result in a reduced stress level due to low water potentials at the cost of reduced water and CO<sub>2</sub> supply. On the other hand, further reducing  $\psi_m$  at the given  $\psi_{pd}$  would result in a dominance of the negative effects ( $\gamma$ ), such as growth inhibition and reduced canopy water supply, and thus lead to a smaller  $\chi$ . Further, Eq. (6) predicts a rapid decline of  $\psi_m$  with decreasing  $\psi_{pd}$  under well-watered conditions, which becomes more gradual and linear as the soil keeps drying (Fig. 1b). This pattern indeed is often observed when studying leaf water potential responses to soil drying<sup>16,17</sup>.

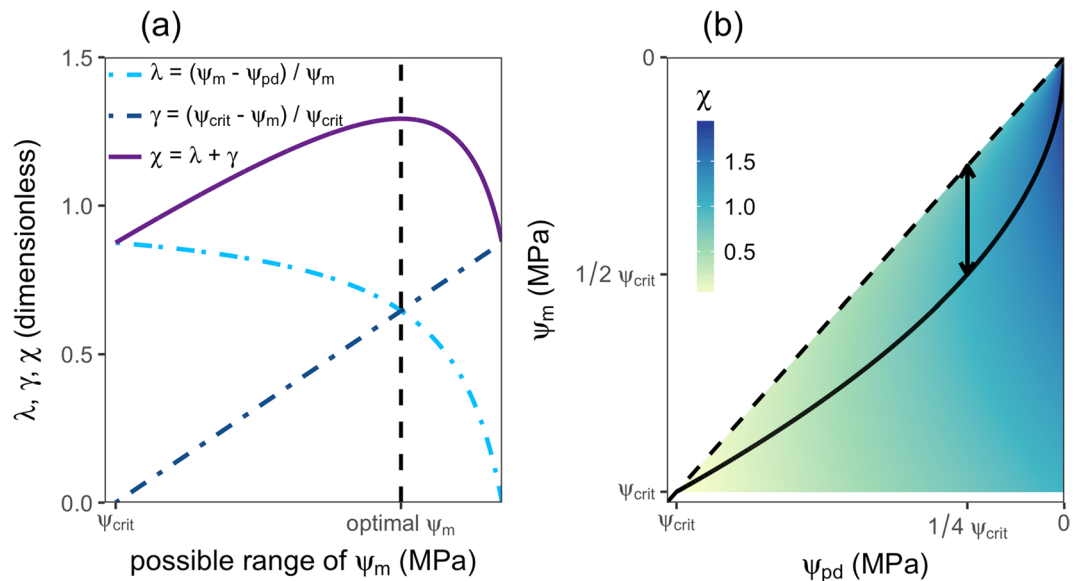


**Figure 1.** Schematic drawing of the described leaf water status optimization. (a) shows an example of how the optimal leaf water potential  $\psi_m$  is found for a given fixed  $\psi_{pd}$  over its entire possible range of leaf water potentials ( $\psi_{crit} < \psi_m < 0$ ). Stress induced by low water potentials (criterion  $\gamma$ ) is least when  $\psi_m$  approaches zero (high  $\gamma$ ) while the water potential gradient maximization criterion  $\lambda$  reaches its maximum as  $\psi_{pd}$  approaches the critical water potential  $\psi_{crit}$ . The optimum leaf water potential for the given  $\psi_{pd}$  is found where  $\chi$  has its maximum (black dashed line) and  $\lambda$  and  $\gamma$  intersect. (b) shows an example of the optimal leaf water potential (approximated by midday water potential,  $\psi_m$ , black solid line) for every possible soil water potential (approximated by predawn water potential,  $\psi_{pd}$ ) ( $\psi_{crit} < \psi_{pd} < 0$ ). The coloring represents the optimization criterion  $\chi$  for any given  $\psi_{pd}$ : the optimal leaf water potential  $\psi_m$  for any given soil water potential  $\psi_{pd}$  is found where  $\chi$  is highest (example for a fixed soil water potential in (a)); the dashed black line represents the one to one line on which the gradient of Eq. (1) vanishes; the arrow represents the point where the rhizosphere to canopy water potential gradient is maximal and at which  $\psi_{pd} = 1/4 \psi_{crit}$  and  $\psi_m = 1/2 \psi_{crit}$ .

Besides predicting the response of  $\psi_m$  to changing  $\psi_{pd}$  the optimal leaf water status regulation model makes two specific predictions. Firstly, the distance between  $\psi_m$  and  $\psi_{crit}$  should monotonically increase as  $\psi_{pd}$  increases and thus stress induced by low leaf water potentials should decrease. The second specific prediction concerns the gradient between the rhizosphere and the canopy ( $\psi_m - \psi_{pd}$ ), which in most instances is the strongest driver of upward water flux through a plant (vertical distance between the solid and the dashed line in Fig. 1b). According to the optimal leaf water status regulation model, this gradient is predicted to be highest at a predawn water potential of  $\psi_{pd} = 1/4 \psi_{crit}$  and correspondingly at midday leaf water potentials of  $\psi_m = 1/2 \psi_{crit}$  ( $d(\psi_m - \psi_{pd})/d\psi_{pd} = 0$ , arrow in Fig. 1b). This implies (everything else being equal) that transpiration should be maximal at intermediate values of  $\psi_m$ , which indeed has been shown to be the case<sup>21</sup>.

The proposed leaf water status regulation model predicts leaf water potentials under the active control of the plant, that is,  $\psi_m > \psi_{crit}$ .  $\psi_m$  may, however, fall below  $\psi_{crit}$  induced by, e.g., cuticular transpiration. As the proposed model is concerned with leaf water status regulation, those values induced by uncontrolled transpiration are beyond the scope of the model.

We acknowledge that this minimal model lumps several processes, such as the relationship between xylem pressure and conductance, into two simple optimization criteria. Yet, we believe that this helps analytically understanding the model without the need to fit many parameters.

## Results

**Comparison of predictions with the database.** The optimal leaf water status regulation model is able to reproduce the initial rapid drop of  $\psi_m$  for high values of  $\psi_{pd}$ , which becomes more gradual with declining  $\psi_{pd}$ , here shown for two exemplary datasets of *Acacia berlandieri* (Fig. 2a) and of *Arbutus unedo* (Fig. 2b), which both homogeneously cover the entire operating range of  $\psi_{pd}$  until  $\psi_{crit}$ .

The overall agreement of model predictions and observations for each dataset in the dryland database is very good, with most of the variance in the data being captured by the model (Fig. 2c,  $R^2 = 0.88$ ) and no systematic bias being apparent from the comparison. Individual model  $R^2$  values are variable but generally in the range of the overall  $R^2$  value (Supplementary Fig. S1, Table S2).

**Comparison of predictions with experimental data.** To perform an independent test of the model's ability to explain observed concurrent reductions of  $\psi_{pd}$  and  $\psi_m$  we applied the model to an experimental dataset<sup>16</sup> using the experimentally determined and the estimated  $\psi_{crit}$  (see Methods) as input to the model.

The model reproduces the overall pattern of concurrent reduction of  $\psi_m$  with  $\psi_{pd}$  well. The underlying functional response of  $\psi_m$  to  $\psi_{pd}$  is shown exemplarily for *Ceanothus cuneatus* (Fig. 3a) and *Salix scouleriana*

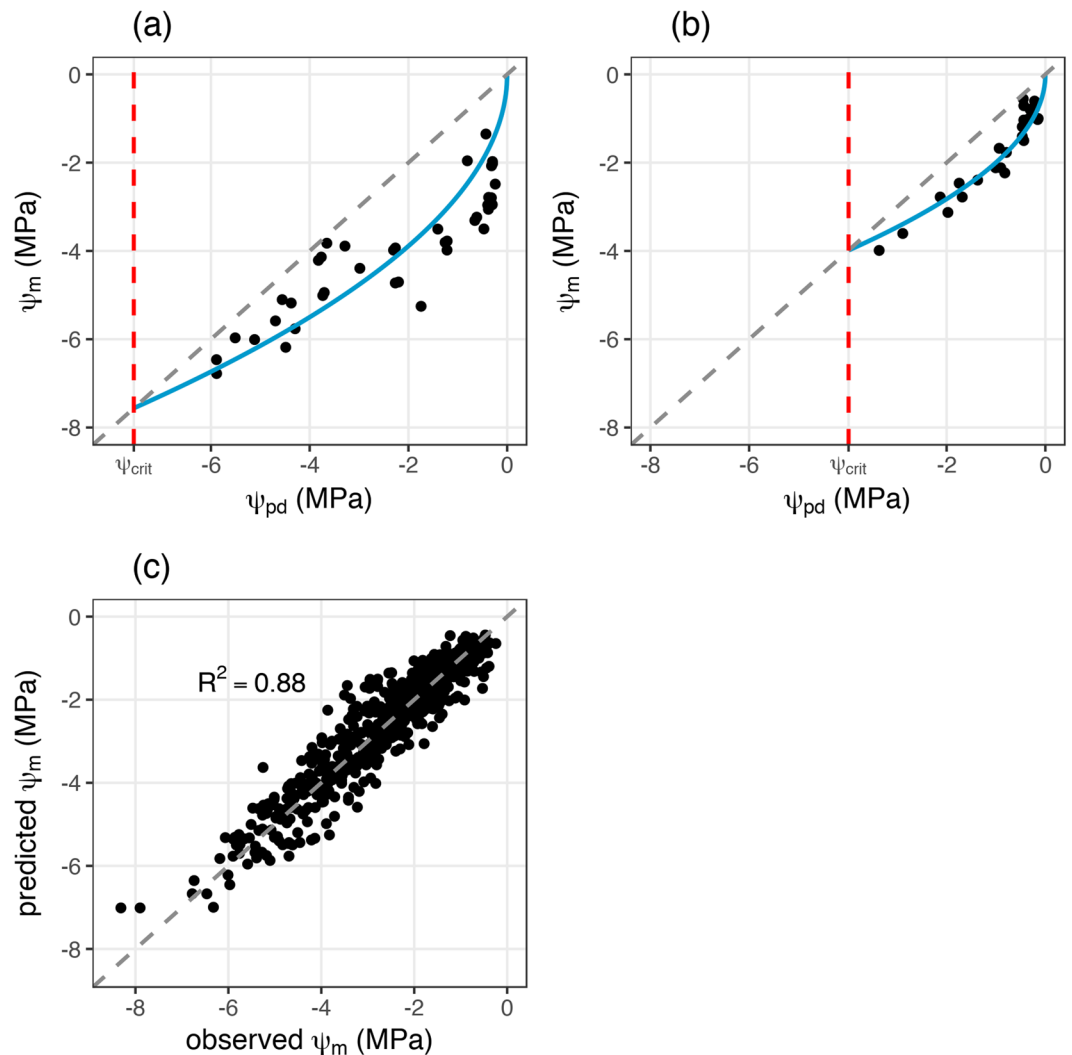


**Figure 2.** Comparison of predictions of the optimal leaf water status regulation model and measured data. Examples of the optimal leaf water status regulation model (blue line) fitted (a) to measured data of *Acacia berlandieri*<sup>22</sup> and (b) to measured data of for *Arbutus unedo*<sup>33</sup>, grey lines in (a,b) are the one to one lines where  $\psi_{pd} = \psi_m$  and the red lines indicate the position of the estimated  $\psi_{crit}$ ; (c) comparison of observed  $\psi_m$  against predicted  $\psi_m$  for all data in the database, the grey dashed line is the one to one line.

(Fig. 3b), which are in the lower and upper end of  $\psi_{crit}$  respectively, of the experimental data. Further comparisons are given in Supplementary Table S1 and Supplementary Figure S4. Also, the overall agreement of model predictions of  $\psi_m$  with observed data is very good (Fig. 3c,  $R^2 = 0.84$ ) and no bias in model predictions can be observed.

To further test the applicability of the model fitting procedure we compared  $\psi_{crit}$  predicted by minimizing the residuals of the model fitted to the experimental data to experimentally determined  $\psi_{crit}$  values (Fig. 3d). The general agreement between both, estimated and observed  $\psi_{crit}$  is good ( $R^2 = 0.6$ ), although particularly for lower values of  $\psi_{crit}$  our model predictions deviate strongly from observations; however, without any bias towards lower or higher values.

**Specific predictions of stress avoidance and hydraulic functioning.** The proposed concept specifically predicts that the effects of stress induced by low leaf water potentials should monotonically decrease as  $\psi_{pd}$  increases. We tested this prediction for two example species from the database (as in Fig. 2a,b) and two example species from the data of the dry-down experiment (as in Fig. 3a,b). The results indeed show that all examples follow the predicted non-linear pattern of stress avoidance closely (Fig. 4, Supplementary Fig. S3a): irrespective of the range of water potentials,  $\psi_{crit} - \psi_m$  declines with declining  $\psi_{pd}$ , with the strongest change in  $\psi_{crit} - \psi_m$  at low stress levels.

The second specific model prediction states that the driving gradient of water flux from the rhizosphere to the canopy (Eq. (1))  $\psi_m - \psi_{pd}$  should be maximal at  $\psi_{pd} = 1/4 \psi_{crit}$  and  $\psi_m = 1/2 \psi_{crit}$ . We compared this hypothesized relationship to the observed pattern (Fig. 5). The observed pattern is less clear and less strongly follows the

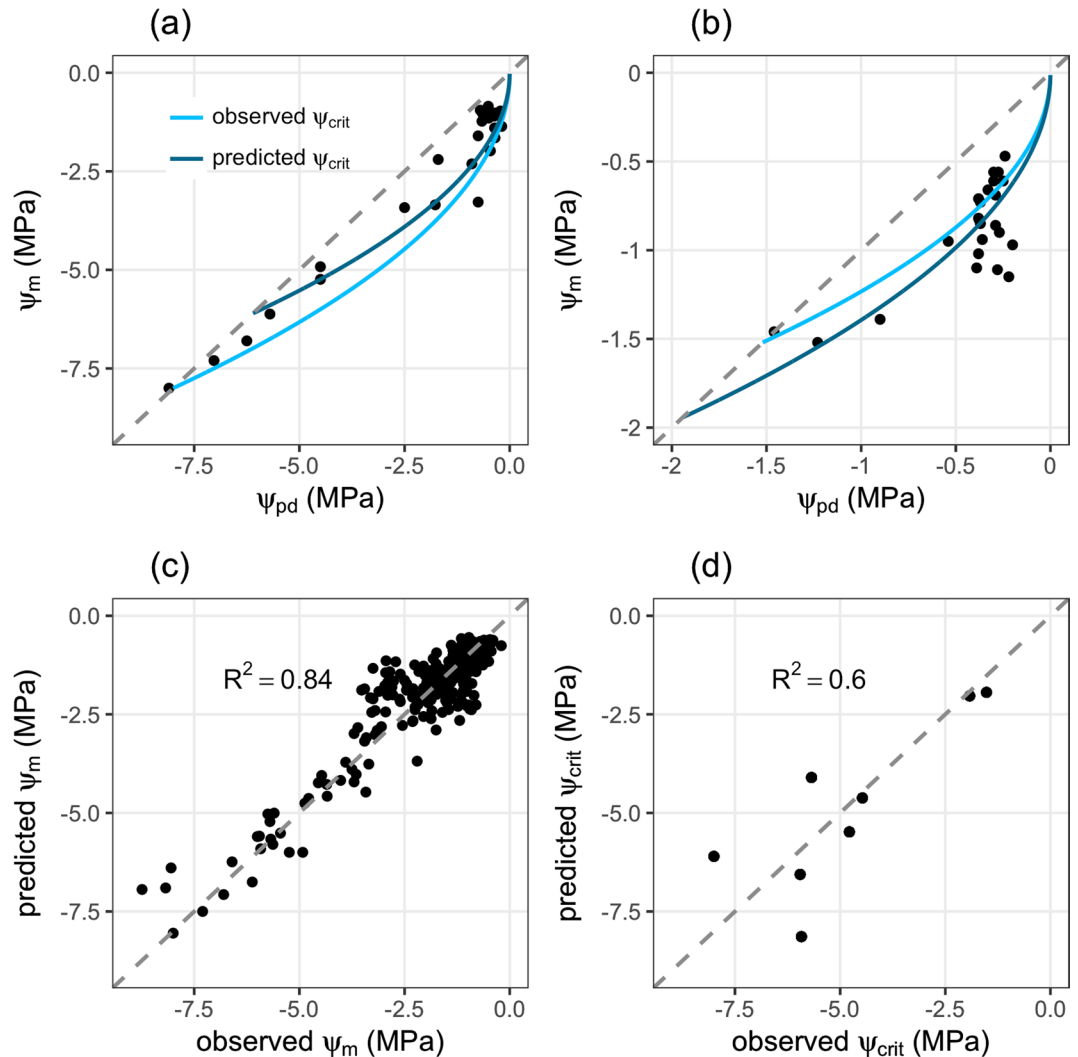


**Figure 3.** Comparison of predictions of the optimal leaf water status regulation model with measured data<sup>16</sup>. Examples of the optimal leaf water status regulation model (solid lines) calculated (a) for *Ceanothus cuneatus* and (b) *Salix scouleriana* based on measured and estimated  $\psi_{crit}$  values, grey lines in (a,b) are the one to one line where  $\psi_{pd} = \psi_m$ . The examples were chosen for two species representing  $\psi_{crit}$  on the upper and lower end, respectively; (c) shows the comparison of observed  $\psi_m$  against predicted  $\psi_m$  (based on measured  $\psi_{crit}$ ) for all data in the experiment, the grey dashed line is the one to one line; (d) shows a comparison of measured  $\psi_{crit}$ <sup>16</sup> (observed) and  $\psi_{crit}$  estimated using residual minimization procedures (see Methods), the grey dashed line is the one to one line.

prediction (Supplementary Fig. S3b) as compared to the first specific prediction (Fig. 4), but is nonetheless apparent: As  $\psi_{pd}$  declines, the gradient  $\psi_m - \psi_{pd}$  rapidly increases until  $\psi_{pd}$  reaches a certain point (Fig. 1b, dashed grey line in Fig. 5). At this point, the water potential gradient between the rhizosphere and the canopy is maximal. As  $\psi_{pd}$  further declines, the gradient  $\psi_m - \psi_{pd}$  decrease again, until it vanishes and  $\psi_{pd} = \psi_m = \psi_{crit}$ . The overall shape of the response of  $\psi_m - \psi_{pd}$  to  $\psi_{pd}$  and its maximum thus follow the predictions made by the presented optimal leaf water status regulation model.

## Discussion

When plants take up CO<sub>2</sub> they are in the dilemma of allowing their leaf water potentials to drop through transpiration while avoiding reduced growth, assimilation and hydraulic conductance through low leaf water potentials. We present a simple model, which formalizes this tradeoff and predicts how plants may optimally solve this problem. We show that optimal leaf water potential regulation indeed appears to be a ubiquitous property of plants of a dryland leaf water potential database. Experimental results moreover indicate optimal leaf water status regulation beyond drylands.

Despite the overall strong agreement between model predictions and observations the model does not capture all variance in the data and does not necessarily explain the variance for all examples better than a simple linear regression. However, as stated in the introduction, our main aim was to describe the tradeoff of leaf water status

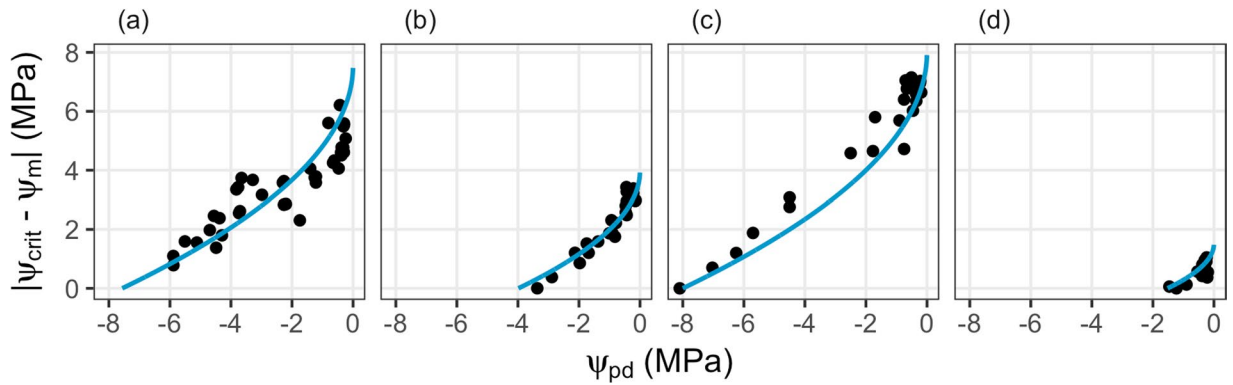


**Figure 4.** Examples of the specific model prediction of stress avoidance, which states that the distance  $\psi_{\text{crit}} - \psi_m$  should increase as  $\psi_{\text{pd}}$  increases. Examples taken are as in Fig. 2 (database, (a) and (b)) and 3 (dry-down experiment, (c,d)): (a) *Acacia berlandieri*, (b) *Arbutus unedo*, (c) *Ceanothus cuneatus* and (d) *Betula scouleriana*. Points are observations, blue lines are model predictions. Model predictions are based on estimated  $\psi_{\text{crit}}$  ((a,b) and measured  $\psi_{\text{crit}}$  (c,d)).

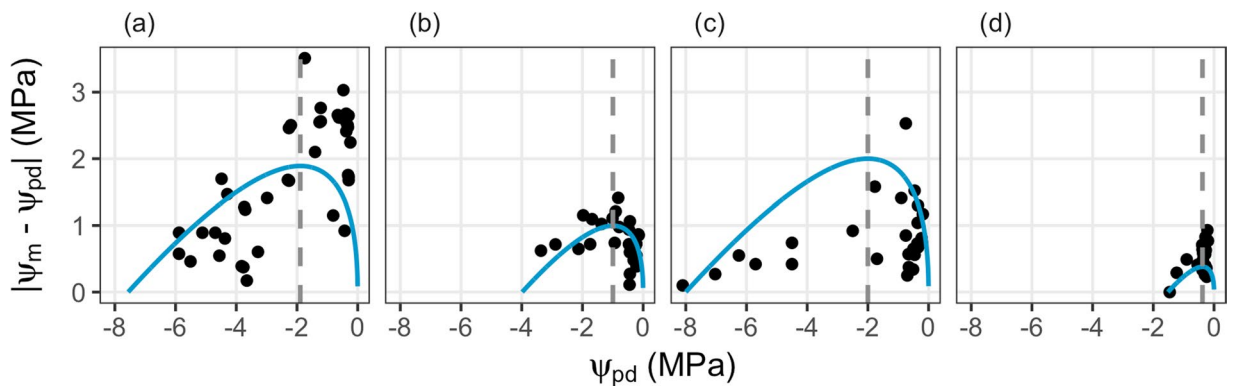


**Figure 5.** Examples of the second specific model prediction stating that the water potential gradient responsible for water flux from the rhizosphere to the canopy,  $\psi_m - \psi_{\text{pd}}$ , should increase as  $\psi_{\text{pd}}$  decreases until a certain point  $\psi_{\text{pd}} = 1/4 \psi_{\text{crit}}$  from which on this gradient decreases again until it reaches  $\psi_{\text{crit}}$ . Examples taken are as in Fig. 2 (database, (a,b)) and 3 (dry-down experiment, (c) and (d)): (a) *Acacia berlandieri*, (b) *Arbutus unedo*, (c) *Ceanothus cuneatus* and (d) *Betula scouleriana*. Points are observations, blue lines are model predictions. Model predictions are based on estimated  $\psi_{\text{crit}}$  ((a,b) and measured  $\psi_{\text{crit}}$  (c,d)).

regulation on a functional rather than a statistical basis, and thus, improving the goodness of fit was not the central point of our analysis. The large overall variance in the data is the result of several factors: Besides water supply, air vapor pressure deficit (VPD) has a strong effect on leaf water potential<sup>22</sup>. This effect is mediated by stomatal conductance, which is proportional to the inverse square root of VPD<sup>23</sup>. Other factors which have an effect on  $\psi_m$  are irradiation as well as changes of the leaf or root area, e.g., through herbivory<sup>24</sup>. Results obtained from the specific model predictions (Eqs (2, 3) and Figs 4, 5) indicate that those deviations from the optimal leaf water status regulation are mainly caused by deviations from the water potential gradient maximization criterion (Eq. (2)), stronger deviations of observations from predictions in Fig. 5 than in Fig. 4, Supplementary Fig. S3). This shows that stress avoidance is a strong driver of optimal leaf water status regulation. On the other hand, maximizing the leaf water supply for a specific soil water supply might not be possible or necessary in all circumstances, such as under high VPD or high irradiation. Despite those deviations, all examples show the predicted maximum of  $|\psi_m - \psi_{\text{pd}}|$  at intermediate values of  $\psi_{\text{pd}}$ , which correspond approximately to the predicted  $1/4 \psi_{\text{crit}}$ . This supports the findings of Manzoni *et al.*<sup>21</sup>, who found maximum transpiration rates at intermediate values of xylem water potential. Our model shows that in addition to the interplay of xylem water potential and conductance, also the gradient between leaf and soil water potential may lead to maximum transpiration at intermediate values of  $\psi_m$ <sup>25</sup>.

The plant trait  $\psi_{\text{crit}}$  is the only parameter to the presented optimal leaf water status regulation model. It is the value of leaf water potentials at which stomata are entirely closed and any decline of  $\psi_m$  beyond this value is likely due to uncontrolled cuticular transpiration. There is evidence that maintaining leaf water potentials above this point prevents the plant from xylem embolism<sup>19,20</sup>. Maintaining  $\psi_m$  above  $\psi_{\text{crit}}$  can, e.g., be achieved by reducing stomatal conductance or by reducing the leaf area. Leaf water potentials around  $\psi_{\text{crit}}$  maintained over longer periods, such as days or weeks, are consequently likely to lead to a partial or complete canopy defoliation<sup>19</sup>. Knowing

$\psi_{\text{crit}}$  can thus help predicting the way how a plant adapts to dry periods: plants that have a comparably high  $\psi_{\text{crit}}$  and thus a narrow operating space for their  $\psi_{\text{m}}$  must balance this through structural adjustments, such as reducing their leaf area<sup>26</sup>. They are more conservative and close their stomata earlier, which will also have a positive effect on soil water availability. On the other hand, plants with lower  $\psi_{\text{crit}}$  will rather adapt physiologically to a drying soil through osmotic adjustments at the leaf level<sup>24</sup>. Although we assume  $\psi_{\text{crit}}$  to be fixed over time in this study, plants in fact may adjust this trait by following water availability<sup>27,28</sup>. Our assumption of plants optimizing their leaf water potential in response to changing soil water potential is therefore rather a matter of hours to days, whereas the adjustment of  $\psi_{\text{crit}}$  happens over weeks or even months<sup>27</sup>.  $\psi_{\text{crit}}$  can thus be expected to be variable over longer time periods, but only within a plant's structural (leaf to root area ratio, leaf morphology, xylem anatomy) and physiological (osmolyte supply) boundaries<sup>24</sup>. The values of  $\psi_{\text{crit}}$  found in this study (Supplementary Fig. S1) are partly lower than the overall minimum  $\psi_{\text{L}}$  at stomatal closure found by Martin-StPaul *et al.*<sup>29</sup>. However, considering that our study focused mainly on dryland species those lower water potentials at stomatal closure might be expected as dry-adaptation. Moreover, they are in the range of  $\psi_{\text{L}}$  at stomatal closure found by Klein<sup>30</sup>.

It is likely that we have under- or overestimated  $\psi_{\text{crit}}$  for several datasets in the dryland database due to the inherent scatter in the water potential trajectories (Figs 2, 3d). Determining the water potential at full stomatal closure is challenging due to the asymptotic nature of the response function of stomatal conductance to  $\psi_{\text{L}}$ <sup>30</sup> and the possible presence of cuticular transpiration. This may have led to relatively low estimates of  $\psi_{\text{crit}}$  (Fig. 2a, Supplementary Figs S1d and S5), which in some cases certainly are below the actual water potential at full stomatal closure. Moreover, if  $\psi_{\text{m}}$  is more strongly controlled by other factors than soil water potential, such as VPD, low  $\psi_{\text{m}}$  at relatively high  $\psi_{\text{pd}}$  values will affect the model fit and consequently the estimated  $\psi_{\text{crit}}$  (Fig. 3b, Supplementary Figs S4 and S5).

We generally advise that those potential issues should be considered when applying the optimal leaf water status regulation model. Ideally, the model should be applied to a dataset where both are available, trajectories of  $\psi_{\text{pd}}$  vs.  $\psi_{\text{m}}$  as well as the water potential at full stomatal closure. If only the latter is known (or a surrogate thereof, such as the leaf water potential at turgor loss<sup>29</sup>) the model can also be applied to simulate the response of leaf water status to soil water availability in a coupled model of plant functioning.

Using a simple model, we found strong support for optimal leaf water status regulation as a fundamental part of plant functioning. These findings contribute to the understanding of how plants regulate their whole hydraulic apparatus and how they may respond to short- and long-term drought stress. Given that our findings and the presented model describe water status regulation of leaves, which form the pivotal link between water supply and demand, it can help elaborating models of whole-plant performance and ecosystem functioning under changing environmental conditions. The proposed model provides a novel view on how plants manage their water balance and provides a way ahead to combine modeling and empirical approaches.

## Methods

**Database.** We compiled a database of concurrent observations of predawn water potential  $\psi_{\text{pd}}$  and midday water potential  $\psi_{\text{m}}$  using primary data published in the peer reviewed scientific literature. The database was established as follows: Following Martínez-Vilalta *et al.*<sup>15</sup> selection criteria for studies to be included were: predawn and midday water potentials were measured concurrently, plants were grown under field conditions (including agricultural fields, but not potted plants), and studies on artificial modifications of plant water potentials were excluded.

We searched Google Scholar for the terms “savanna” + “leaf water potential” as well as “dryland” + “leaf water potential”. We also followed the database compiled by Martínez-Vilalta *et al.*<sup>15</sup>, and extracted data points for studies listed in their literature table. All data points were extracted from the original articles using WebPlotDigitizer (<https://automeris.io/WebPlotDigitizer>).

We focused on studies conducted in dry environments since water potentials in water-limited environments are likely to span a wider range. An aridity index (mean annual precipitation divided by mean annual potential evapotranspiration) was used as a decision criterion whether a study site was considered dry or not. Only locations which have an aridity index smaller 0.75 were regarded as drylands<sup>31</sup>. To this end, only studies reporting the explicit coordinates of the study location or allowing for their reconstruction were considered. If a study reported different study locations, they were only treated separately if their distinct coordinates were available. The aridity index at a given site was then extracted using the dataset of<sup>32</sup>.

For a given site, data points were aggregated at the species level, but not on the sub-species level. If data for the same species were found for different locations, those data points were treated separately. This was deemed necessary as a variable  $\psi_{\text{crit}}$  can be an intraspecific adaptation to different environments<sup>28</sup>. An overview of the different locations for which data were extracted is shown in Supplementary Fig. S2.

To base the analyses on a reliable basis, we only considered datasets with at least seven concurrent measurements of  $\psi_{\text{pd}}$  and  $\psi_{\text{m}}$ . Additionally, to obtain a robust model fit, we only considered datasets that covered at least 25% of the distance between 0 MPa and  $\psi_{\text{crit}}$  (Supplementary Fig. S1, value *rel\_range* in Supplementary Table S2). We used this post-hoc criterion to omit datasets, for which the range of available data was too small to make reliable predictions of  $\psi_{\text{crit}}$ . The cut-off threshold of 25% was selected based on the observation that above this value  $R^2$  values of most model fits were positive, while for lower values  $R^2$  was often negative (Supplementary Fig. S1). We deemed an  $R^2$  larger 0 as a criterion for a good model fit, since this indicates that the model captures more than the variance captured by the mean. The  $R^2$  was calculated as 1 minus model residual sum of squares relative to the residual sum of squares to the mean. This additional post-hoc criterion resulted in a total removal of 15 datasets initially included in the analysis. The literature search and database compilation resulted in 28 publications that were included in the analysis (Supplementary Tables S2 and S3). From those studies, a total of 43 unique datasets containing 38 species were extracted. Each data set consists of on average 16 observations. The database covers a

wide range of leaf water potentials stretching from  $-6.6$  MPa to  $-0.03$  for  $\psi_{pd}$  and from  $-8.3$  MPa to  $-0.2$  MPa for  $\psi_m$  (Fig. 2, Supplementary Table S2).

The data collected in this database span several time periods ranging from days to months and sometimes include data which were averaged over several individuals. To test the presented concept across several species over a fixed time span under controlled conditions comprising a single soil dry-down experiment, we additionally used data published in Meinzer *et al.*<sup>16</sup>.  $\psi_{pd}$  and  $\psi_m$  of eight woody species (Supplementary Table S1) were measured during the dry-down experiment until  $\psi_m$  equaled  $\psi_{pd}$ . This was then assumed to be the critical water potential  $\psi_{crit}$ . The range of water potentials covered by the experimental data is similar to the range covered by all other datasets in our new database with minimum  $\psi_{pd}$  of  $-8.1$  MPa and maximum  $\psi_{pd}$  of  $-0.15$  MPa, as well as minimum  $\psi_m$  of  $-8.74$  MPa and maximum  $\psi_m$  of  $-0.2$  MPa. For a more detailed description of the experiment see Meinzer *et al.*<sup>16</sup>.

**Application of the model.** We fitted the model describing the optimal leaf water status regulation (Eq. (6)) to each single data set (separated by species and location) by determining  $\psi_{crit}$  that minimizes the residual sum of squares of the predicted versus the measured data. Specifically, we selected the  $\psi_{crit}$  from a range of water potentials between  $-15$  to  $-0.05$  MPa with a total length of 1000 numbers that minimized the residual sum of squares for each unique dataset.

We further compared  $\psi_{crit}$  values measured during the dry-down experiment<sup>15</sup> to the one obtained by minimizing the residuals of our model.

Data shown for the global dryland database do not comprise the data of the dry-down experiment.

All data of the database are available in Supplementary Table S2.

## References

- Jarvis, P. G. The interpretation of the variations in leaf water potential and stomatal conductance found in canopies in the field. *Phil. Trans. R. Soc. Lond. B* **273**, 593–610 (1976).
- Oertli, J. J. The Soil – Plant – Atmosphere Continuum. In *Water and Plant Life* (eds Lange, O. L., Kappen, L. & Schulze, E.-D.) **19**, 32–41 (Springer 1976).
- Zimmermann, M. H. *Xylem Structure and the Ascent of Sap*. (Springer 1983).
- Hsiao, T. C. Plant Responses to Water Stress. *Ann. Rev. Plant Physiol.* **24**, 519–570 (1973).
- Slatyer, R. O. *Plant-Water Relationships*. (Academic Press 1967).
- Sperry, J. S., Adler, F. R., Campbell, G. S. & Comstock, J. P. Limitation of plant water use by rhizosphere and xylem conductance: results from a model. *Plant Cell Environ.* **21**, 347–359 (1998).
- Buckley, T. N. The control of stomata by water balance. *New Phytol.* **168**, 275–292 (2005).
- Muller, B. *et al.* Water deficits uncouple growth from photosynthesis, increase C content, and modify the relationships between C and growth in sink organs. *J. Exp. Bot.* **62**, 1715–1729 (2011).
- Fatichi, S., Leuzinger, S. & Koerner, C. Moving beyond photosynthesis: from carbon source to sink-driven vegetation modeling. *New Phytol.* **201**, 1086–1095 (2014).
- Larcher, W. *Physiological Plant Ecology*. (Springer 2003).
- Tyree, M. T. & Ewers, F. W. The hydraulic architecture of trees and other woody plants. *New Phytol.* **119**, 345–360 (1991).
- Wolf, A., Anderegg, W. R. L. & Pacala, S. W. Optimal stomatal behavior with competition for water and risk of hydraulic impairment. *Proc. Natl. Acad. Sci. USA* **113**, E7222–E7230 (2016).
- Sperry, J. S., Hacke, U. G., Oren, R. & Comstock, J. P. Water deficits and hydraulic limits to leaf water supply. *Plant Cell Environ.* **25**, 251–263 (2002).
- Meinzer, F. Functional convergence in plant responses to the environment. *Oecologia* **134**, 1–11 (2003).
- Martinez-Vilalta, J., Poyatos, R., Aguadé, D., Retana, J. & Mencuccini, M. A new look at water transport regulation in plants. *New Phytol.* **204**, 105–115 (2014).
- Meinzer, F. C. *et al.* Mapping ‘hydrosapes’ along the iso- to anisohydric continuum of stomatal regulation of plant water status. *Ecol. Lett.* **19**, 1343–1352 (2016).
- Kaufmann, M. R. Water Relations of Pine Seedlings in Relation to Root and Shoot Growth. *Plant Physiol.* **43**, 281–288 (1968).
- Warren, C. R., Livingston, N. J. & Turpin, D. H. Responses of gas exchange to reversible changes in whole-plant transpiration rate in two conifer species. *Tree Physiol.* **23**, 793–803 (2003).
- Hochberg, U. *et al.* Stomatal Closure, Basal Leaf Embolism, and Shedding Protect the Hydraulic Integrity of Grape Stems. *Plant Physiol.* **174**, 764–775 (2017).
- Brodribb, T. J. *et al.* Visual quantification of embolism reveals leaf vulnerability to hydraulic failure. *New Phytol.* **209**, 1403–1409 (2016).
- Manzoni, S. *et al.* Hydraulic limits on maximum plant transpiration and the emergence of the safety-efficiency trade-off. *New Phytol.* **198**, 169–178 (2013).
- Rodríguez, H. G., Silva, I. C., Meza, M. G. & Jordan, W. R. Seasonal Plant Water Relationships in *Acacia berlandieri*. *Arid Soil Res. Rehab.* **14**, 343–357 (2000).
- Medlyn, B. E. *et al.* Reconciling the optimal and empirical approaches to modelling stomatal conductance. *Global Change Biol.* **17**, 2134–2144 (2011).
- McNaughton, S. J. Dryland Herbaceous Perennials. In *Response of Plants to Multiple Stresses* (eds Mooney, H. A., Winner, W. E. & Pell, E. J.) 307–328 (1991).
- Jones, H. G. & Sutherland, R. A. Stomatal control of xylem embolism. *Plant Cell Environ.* **14**, 607–612 (1991).
- Meinzer, F. C. & Grantz, D. A. Stomatal and hydraulic conductance in growing sugarcane: stomatal adjustment to water transport capacity. *Plant Cell Environ.* **13**, 383–388 (1990).
- Kolb & Sperry. Transport constraints on water use by the Great Basin shrub, *Artemisia tridentata*. *Plant Cell Environ.* **22**, 925–935 (1999).
- Bartlett, M. K. *et al.* Global analysis of plasticity in turgor loss point, a key drought tolerance trait. *Ecol. Lett.* **17**, 1580–1590 (2014).
- Martin-StPaul, N., Delzon, S. & Cochard, H. Plant resistance to drought depends on timely stomatal closure. *Ecol. Lett.* **20**, 1437–1447 (2017).
- Klein, T. The variability of stomatal sensitivity to leaf water potential across tree species indicates a continuum between isohydric and anisohydric behaviours. *Funct. Ecol.* **28**, 1313–1320 (2014).
- Whitford, W. G. *Ecology of Desert Systems*. (Academic Press 2002).
- Trabucco, A. & Zomer, R. J. *Global Aridity Index (Global-Aridity) and Global Potential Evapo-Transpiration (Global-PET) Geospatial Database* (2009).
- Castell, C., Terradas, J. & Tenhunen, J. D. Water relations, gas exchange, and growth of resprouts and mature plant shoots of *Arbutus unedo* L. and *Quercus ilex* L. *Oecologia* **98**, 201–211 (1994).



## Acknowledgements

We thank Lena Dressler for her help with compiling the database. We are also grateful to Frederick Meinzer and his colleagues for sharing their dataset. This work was supported by the German Federal Ministry of Education and Research (BMBF) project OPTIMASS (01LL1302B).

## Author Contributions

G.R. and B.T. conceived and designed the study; G.R. and L.Z. compiled the database; G.R. analyzed the data and drafted the manuscript; G.R. and B.T. contributed to elaborating and editing the manuscript.

## Additional Information

**Supplementary information** accompanies this paper at <https://doi.org/10.1038/s41598-019-40448-2>.

**Competing Interests:** The authors declare no competing interests.

**Publisher's note:** Springer Nature remains neutral with regard to jurisdictional claims in published maps and institutional affiliations.



**Open Access** This article is licensed under a Creative Commons Attribution 4.0 International License, which permits use, sharing, adaptation, distribution and reproduction in any medium or format, as long as you give appropriate credit to the original author(s) and the source, provide a link to the Creative Commons license, and indicate if changes were made. The images or other third party material in this article are included in the article's Creative Commons license, unless indicated otherwise in a credit line to the material. If material is not included in the article's Creative Commons license and your intended use is not permitted by statutory regulation or exceeds the permitted use, you will need to obtain permission directly from the copyright holder. To view a copy of this license, visit <http://creativecommons.org/licenses/by/4.0/>.

© The Author(s) 2019